Published in final edited form as:
Cell Host Microbe. 2010 November 18; 8(5): 445–454. doi:10.1016/j.chom.2010.10.005.

Statins Enhance Formation of Phagocyte Extracellular Traps

Ohn A. Chow[1,2,4,†], **Maren von Köckritz-Blickwede**[1,†], **A. Taylor Bright**[4], **Mary E. Hensler**[1], **Annelies S. Zinkernagel**[1], **Anna L. Cogen**[3], **Richard L. Gallo**[1,3,6], **Marc Monestier**[7], **Yanming Wang**[8], **Christopher K. Glass**[2,3,4,*], and **Victor Nizet**[1,5,9,*]

[1] Department of Pediatrics, University of California, San Diego, La Jolla, California 92093, USA

[2] Department of Cellular and Molecular Medicine, University of California, San Diego, La Jolla, California 92093, USA

[3] Department of Medicine, University of California, San Diego, La Jolla, California 92093, USA

[4] Biomedical Sciences Graduate Program, University of California, San Diego, La Jolla, California 92093, USA

[5] Skaggs School of Pharmacy and Pharmaceutical Sciences, University of California, San Diego, La Jolla, California 92093, USA

[6] Veterans Administration San Diego Health Care System, Pennsylvania, 16802

[7] Department of Microbiology and Immunology and Temple Autoimmunity Center, Temple University School of Medicine, Pennsylvania, 16802

[8] Department of Biochemistry and Molecular Biology, Pennsylvania State University, University Park, Pennsylvania, 16802

[9] Rady Children's Hospital, San Diego, California 92123, USA

SUMMARY

Statins are inhibitors of 3-hydroxy 3-methylglutaryl coenzyme A (HMG-CoA) reductase, the rate-limiting enzyme in cholesterol biosynthesis. Several recent clinico-epidemiologic studies have revealed that patients receiving statin therapy have reduced mortality associated with severe bacterial infection. Here we study pharmacological effect of statins on the innate immune capacity of phagocytic cells, focusing on the leading human bacterial pathogen *Staphylococcus aureus*. These studies revealed a beneficial effect of statins on *S. aureus* clearance using *in vivo*, *ex vivo* and *in vitro* models of phagocyte function, although paradoxically both phagocytosis and oxidative burst were inhibited. Probing instead for an extracellular mechanism of killing, we found statins boosted the production of anti-bacterial DNA-based extracellular traps (ETs) by human and murine neutrophils and also monocyte/macrophages. The effect of statins to induce phagocyte ETs was linked to sterol pathway inhibition by RNA interference and specific pharmacologic inhibitors. We conclude that a drug therapy taken chronically by tens of millions of individuals alters the functional behavior of phagocytic cells, which could have ramifications for susceptibility and response to bacterial infections in these patients.

[*]Correspondence: ckg@ucsd.edu (C.K.G.) or vnizet@ucsd.edu (V.N.).
[†]These authors contributed equally.

INTRODUCTION

Statins are inhibitors of 3-hydroxy 3-methylglutaryl coenzyme A (HMG-CoA) reductase, the rate-limiting enzyme in cholesterol biosynthesis. The mainstay of current hyperlipidemia treatment, an estimated 30 million individuals were prescribed statins in 2005 in the U.S. alone (Stagnitti, 2008.). The prevalence of statin usage has stimulated great interest to identify and understand significant biological effects of these drugs beyond cholesterol lowering (Merx and Weber, 2008). One remarkable observation to emerge from several clinico-epidemiological studies is that patients receiving statin therapy may experience reduced infection-associated mortality due to pneumonia (Thomsen et al., 2008), bacteremia (Kruger et al., 2006; Liappis et al., 2001) or sepsis (Almog et al., 2007; Kopterides and Falagas, 2009; Martin et al., 2007). Consistent with this finding, statin therapy improved survival in mouse sepsis models including lipopolysaccharide (LPS) administration (Ando et al., 2000), cecal ligation and perforation (CLP) (Merx et al., 2005; Merx et al., 2004), or systemic challenge with Gram+ or Gram− bacteria (Catron et al., 2004; Chaudhry et al., 2008).

The mechanism(s) by which statin treatment may protect against lethal bacteremia and sepsis are not yet understood. Certain statins exhibit modest inhibitory activity against bacterial growth *in vitro*, e.g. MIC 30 mg/L vs. *Staphylococcus aureus* for simvastatin (Jerwood and Cohen, 2008), but the drug level required for this effect (30 mg/L = 70 μM) exceeds by ~300-fold the serum level reported in the experimental mouse model following high dose therapy (220 nM with 100 mg/kg/day simvastatin orally) (Thelen et al., 2006). Rather, more attention has focused on immunomodulatory effects of statins that could reduce the pro-inflammatory “cytokine storm” of sepsis. Statin-treated mice had decreased tumor necrosis factor-α (TNFα) and interleukin-1β (IL-1β) or IL-6 levels upon LPS challenge (Ando et al., 2000; Chaudhry et al., 2008), and statin-treated human volunteers receiving LPS also had lower serum TNFα and IL-1β levels, coupled with diminished monocyte Toll-like receptor-4 (TLR-4) and TLR-2 expression (Niessner et al., 2006). Peripheral blood mononuclear cells (PBMC) isolated from statin-treated humans showed diminished TNFα and IL-6 responses to LPS *ex vivo* (Rosenson et al., 1999), and statin exposure blunted LPS-induced TNFα, IL-1β, IL-6 and inducible nitric oxide synthase (iNOS) expression by rat macrophages *in vitro* (Pahan et al., 1997).

Here we consider an alternative mechanism by which statins could influence the outcome of bacterial infection – by altering the intrinsic innate immune (bactericidal) capacity of phagocytic cells. We find that statin therapy *in vitro*, *ex vivo* and *in vivo* increases the ability of phagocytes to kill the leading human pathogen *S. aureus*, a phenotype we correlate to increased production of antimicrobial DNA-based extracellular traps. This alteration in immune cell behavior is mediated by inhibition of the sterol pathway.

RESULTS

Statin Induction of Phagocyte Antimicrobial Activity *In Vitro*

We first tested the effect of *in vitro* stimulation with the classical HMG-CoA reductase inhibitor mevastatin on the ability of various phagocytic cell types to kill *S. aureus*. Statin pre-treatment significantly increased the anti-staphylococcal activity of human neutrophils, human U937 monocyte/macrophages, and murine RAW 264.7 macrophages (Figure 1A). At the concentration used, mevastatin had no direct effect on *S. aureus* growth (Figure 1B), nor did pretreatment of *S. aureus* with mevastatin render the bacterium more susceptible to killing by normal neutrophils (Figure 1C). Statin enhancement of human neutrophil killing of *S. aureus* was observed in assays performed with our without prior opsonization of the bacteria using autologous serum (Figure 1D). Statin treatment enhanced RAW 264.7

macrophage clearance of strains of methicillin-resistant *S. aureus* (MRSA), group B *Streptococcus*, *Salmonella typhimurium*, and *Streptococcus pneumoniae*, suggesting the induction of a generalized mechanism(s) for bacterial killing (Figure 1E).

In beginning to probe the mechanism by which statin treatment could enhance leukocyte bactericidal function, we were presented with a paradox. Previous literature suggested that statin treatment of neutrophils and macrophages was associated with reduction in phagocytosis and oxidative burst, two key effectors of bacterial killing (Benati et al., 2009; Bokoch and Prossnitz, 1992). We confirmed that mevastatin treatment reduced phagocytic uptake of fluorescently-labelled *S. aureus* by human neutrophils as measured by FACS (Figure 1F) and reduced the magnitude of the neutrophil oxidative burst elicited by *S. aureus* infection (Figure 1G). These observed inhibitory effects on phagocytosis and oxidative burst suggested statin treatment was stimulating a mechanism for extracellular bacterial killing. Consistent with this hypothesis, we found that enhanced killing of *S. aureus* by statin-treated neutrophils was maintained in the face of treatment with cytochalasin D (Figure 1H), an actin microfilament inhibitor that blocks bacterial uptake (Figure 1F).

Statin Induction of Neutrophil Extracellular Traps (NETs)

A key emerging concept in neutrophil biology is antimicrobial activity achieved through the elaboration of neutrophil extracellular traps (NETs) (Brinkmann et al., 2004). The product of a novel cell death pathway, NETs are composed of nuclear DNA, histones, antimicrobial peptides and proteases, and are capable of entrapping and killing a wide variety of bacteria and other microbes (Brinkmann and Zychlinsky, 2007; von Kockritz-Blickwede and Nizet, 2009). We found that mevastatin treatment *in vitro* strikingly enhanced NET production by freshly-isolated and PMA-stimulated human neutrophils (Figures 2A and 2B). Histones and cathelicidin antimicrobial peptide LL-37, two of the key antimicrobial effectors present in NETs (Brinkmann and Zychlinsky, 2007; von Kockritz-Blickwede and Nizet, 2009), were also released in greater amounts following statin treatment and co-localized within the NETs (Figures 2A and 2B). Quantifying NETs by direct assessment of extracellular DNA release (Fuchs et al., 2007), we calculated mevastatin-treated neutrophils produced 2.5-fold more NETs (Figure 2C), leading to greater entrapment of fluorescently labeled *S. aureus* within these structures (Figure 2D). We found that lovastatin, simvastatin and fluvastatin also enhanced NET production, demonstrating that this phenomenon is not limited to mevastatin and is common across the statin class of drugs (Figure 2E). Consistent with a specific NET-dependent killing mechanism, the mevastatin-induced enhancement of neutrophil bacterial killing was abrogated if neutrophils were lysed mechanically using sonication (Figure S1A) or if exogenous micrococcal nuclease treatment was used to degrade NETs (Figure S1B).

NET release has previously been reported to depend upon reactive oxygen species (ROS) generation through the NAPDH oxidase. When we blocked neutrophil ROS production using the NADPH oxidase inhibitor diphenylene iodonium (DPI), the level of NET generation was clearly reduced, yet still significantly greater in statin-treated cells vs. controls (Figure 2F). Combined with the observation that statin treatment reduced overall ROS production in the neutrophils (Figure 1G), the evidence suggests that statins may predispose cells to enter the NET cell death pathway in response to a lower threshold level of ROS signal. Another biochemical marker of NET formation identified in response to LPS or ROS is deimination of arginine residues in histones to citrullines, a post-translational modification catalyzed by peptidyl arginine deaminase 4 (PAD-4) that facilitates chromatin decondensation (Wang et al., 2009). However, we found that in contrast to control neutrophils, treatment with an inhibitor of PAD-4-mediated histone citrullination failed to block the increased NET production associated with mevastatin or simvastatin treatment (Figures S2A and S2B).

Statin-Induction of Macrophage Extracellular Traps (METs)

Statin enhancement of *S. aureus* killing was not restricted to human neutrophils, but was also observed in macrophages/monocytes (Figure 1A). Similar to our findings with neutrophils, statin treatment of RAW 264.7 macrophages reduced phagocytic uptake of *S. aureus* (Figure S3). Unlike neutrophils, eosinophils or mast cells (von Kockritz-Blickwede et al., 2008), release of nuclear DNA to form extracellular traps has never been reported for macrophages. However, we found a subset of macrophages capable upon PMA stimulation to elaborate extracellular DNA to form NET-like structures we now refer to as macrophage extracellular traps (METs). Like NETs, RAW 264.7 METs could be readily visualized with DNA stains such as DAPI and/or in combination with antibodies against histone-DNA-complexes, and were increased by 2.2-fold in statin-treated cells vs. controls (Figure 3A). Using mammalian cell viability staining, we found that formation of METs, as previously reported for neutrophils and mast cells, is associated with death of the cell (Figure 3B). The percentage of MET-producing cells (Figure 3A) correlated will with the percentage of dead cells (Figure 3B). Using the Baclight Live/Dead viability assay, we found that the great majority of FITC-labelled *S. aureus* entrapped within METs were nonviable as indicated by red staining (Figure 3D). This finding suggests that, similar to NETs, METs can subserve an innate immune function. The murine cathelicidin peptide CRAMP was visualized within MET structures induced by statin treatment in RAW 264.7 cells (Figure S4A). Similarly, we found that statin treatment could elicit production of DNA-based extracellular traps from thioglycolate-elicited murine peritoneal macrophages (Figure S4B).

Statin Therapy *In Vivo* Enhances Phagocyte Bactericidal Activity

To extend our observations to statin treatment of the whole animal, thioglycolate-stimulated peritoneal cells were extracted and purified from mice that had been pre-fed with standard chow supplemented with or without simvastatin. In both groups of mice, the composition of the peritoneal cell population was 60–70% neutrophils and 10–20% mononuclear cells (Figure 4A). In good correlation to the *in vitro* data, the peritoneal cells from simvastatin-treated mice showed increased production of extracellular traps (Figure 4B) as well as enhanced killing of *S. aureus* compared to peritoneal cells isolated from control mice (Figure 4C).

Protective Effect of Statin Therapy Against *Staphylococcus aureus* Pneumonia

To determine the effects of statin therapy on resistance to infection, we used an established intranasal inoculation model of *S. aureus* pneumonia that has been shown to mirror several clinical and pathological features of human bacterial pneumonia (Bubeck Wardenburg et al., 2007; Bubeck Wardenburg and Schneewind, 2008). In this model, mice challenged with a sublethal dose of *S. aureus* ($1–2 \times 10^8$ cfu/animal) develop histopathological evidence of lung organ damage between 24 and 72 h of infection (Bubeck Wardenburg et al., 2007). In comparison to mice fed standard chow, we found that mice fed chow supplemented with simvastatin showed reduced bacterial levels in the lung 48 h post-challenge (Figure 4D). Histopathological changes characteristic of severe bacterial pneumonia were diminished in simvastatin-treated mice. Whereas the majority of bronchi and alveolar spaces were obliterated by inflammatory exudates, immune cell infiltrates, and staphylococci in control mice (Figure 4E, top), the simvastatin-treated group exhibited smaller, discrete areas of inflammation, surrounded by large unaffected areas of lung tissue (Figure 4E, bottom). Recruitment of a mixed population of neutrophils and macrophages was evident in the inflammatory lesions of both groups. To determine if the effect of statin treatment to enhance extracellular trap production was operating *in vivo*, we also examined lung sections for extracellular traps. In correlation with our in vitro data, significantly more extracellular traps (~7-fold increase), enriched in the cathelicidin peptide CRAMP, were found in the simvastatin-treated group (Figure 4F, 4G and Figure S5A, S5B). Many of the extracellular

traps from simvastatin-treated mice were quite large and extended into the alveolar space (Figure 4F and Figure S5A), whereas traps from control mice were small and localized to the alveolar wall. While the more severe degree of inflammation and pneumonia in control mice vs. simvastatin-treated mice precludes a meaningful analysis by total levels, immunofluorescence for CRAMP expression on a per cell basis (CRAMP/DAPI ratio, calculated from the data shown Figure S5B) was significantly greater in simvastatin-treated animals (1.01 ± 0.12) than controls (0.87 + 0.16, $P < 0.001$).

Inhibition of Sterol Production Stimulates the Formation of Phagocyte Extracellular Traps

We next sought to determine the relationship between the mevalonate pathway for cholesterol biosynthesis, which statins target medically, and the observed effect of these drugs to boost phagocyte antibacterial function. Effective inhibition of HMG-CoA reductase by siRNA knockdown of Hmgcr in thioglycolate-induced murine peritoneal macrophages (Figure 5A) was sufficient to enhance both their production of METs (Figure 5B and 5C) and their killing of *S. aureus* (Figure 5D), suggesting that statin treatment was not exerting an off-target effect. Moreover, addition of an excess of the downstream HMG-CoA reductase product mevalonate almost completely blocked the bactericidal enhancing properties of statin therapy on macrophages (1 mM mevalonate shown in Figure 5E; 250 μM mevalonate shown in Figure S6A), without exerting a cytotoxic effect on the cells (Figure S6B).

The mevalonate pathway is involved in a number of cellular processes including protein prenylation and cholesterol synthesis (Figure 6A). A critical juncture is the processing of farnesyl pyrophosphate (FPP), which can be used in protein prenylation pathways, such farnesylation or geranylgeranylation, or committed to the cholesterol synthetic pathway by conversion to squalene. To pinpoint which of these branch pathways mediates NET induction by statins, we performed NET quantitation assays following treatment with inhibitors against farnesyl transferase (FTI-277), geranylgeranyl transferase (GGTI-298) and squalene synthase (YM-53601). We found that YM-53601 induced NETs to a level similar to mevastatin treatment (Figures 6B and 6C), whereas GGTI-298 only resulted in a very small increase, and FTI-277 had no effect (Figure 6B). As observed with statins, treatment of neutrophils with YM-53601 resulted in enhanced clearance of *S. aureus* (Figures 6D and 6E). These data suggest the effects of statins in boosting NET production and bacterial killing are mediated by intermediates of the sterol synthetic pathway.

DISCUSSION

Our results demonstrate that statin treatment to inhibit the sterol pathway fundamentally alters the innate immune behavior of phagocytic cells. In response to the leading bacterial pathogen *S. aureus*, we found statin to enhance formation of phagocyte ETs and promote bacterial killing. This phenotypic effect may function synergistically with cytokine modulation to help explain human clinical data pointing to a lower risk of severe bacterial infection and sepsis in patients receiving statin therapy (Almog et al., 2007; Kopterides and Falagas, 2009; Kruger et al., 2006; Liappis et al., 2001; Martin et al., 2007; Thomsen et al., 2008) and the therapeutic benefits of statins observed in mice challenged systemically with *S. aureus* or *Salmonella typhimurium* (Catron et al., 2004; Chaudhry et al., 2008). The fact that statins show a protective effect in animals receiving LPS challenge alone reflects the importance of their immunomodulatory properties (Ando et al., 2000).

The formation of ETs by phagocytic cells has been shown to not only exert antibacterial effects but also to provoke inflammation, and pathological release of ETs appears to play a role in inflammatory disease conditions such as autoimmune vasculitis and lupus nephritis (Gupta et al.; Hakkim et al.; Kessenbrock et al., 2009). In the case of *S. aureus*, excessive

neutrophil recruitment to the lung, mediated in part by its secreted alpha-toxin, is a contributor to lung tissue injury and disease pathology (Bartlett et al., 2008). It is notable that *S. aureus* is capable of triggering the rapid necrotic lysis of neutrophils after its own phagocytic uptake (Kobayashi et al., 2010). Thus while release of NETs in response to *S. aureus* lung infection may provoke local inflammation, this calculated "sacrifice" of the neutrophil could have a more favorable ratio of antibacterial effect to inflammatory consequences than pathogen-mediated necrotic neutrophil lysis.

Beyond histopathological images of entrapped bacteria, *in vivo* evidence that ETs play an important role in innate immunity is derived from studies that show increased virulence of pathogens capable of producing endonucleases that degrade ETs (Beiter et al., 2006; Buchanan et al., 2006; Walker et al., 2007), decreased virulence of bacterial strains expressing surface structures that promote entrapment within ETs (Crotty Alexander et al. 2010), or a therapeutic benefit of nuclease inhibitors in ET preservation at foci of acute infection (Buchanan et al., 2006). The present study contributes additional circumstantial evidence for an important role of ETs in host antibacterial defense, and may help explain a decades old study that provided clear evidence that an "as yet unidentified" nonphagocytic, extracellular killing mechanism was critical to control of *S. aureus* pneumonia in the murine model (Nugent and Pesanti, 1982). And while our studies confirm earlier observations that statin therapy inhibits phagocytotic uptake of bacteria by neutrophils and macrophages (Figure 1F, Figure S3), prior opsonization of the bacteria increased overall killing by statin-treated neutrophils (Figure 1D), hinting that other innate antibacterial activities of the phagocytic cells could be statin-responsive. Revealing further complexity and interdependence of extracellular and intracellular killing mechanisms, prior opsonization and phagocytotic uptake of *Candida albicans* have each been reported to increase NET production (Urban et al. 2006).

The ultimate effect of statin induction of ET formation on host immune clearance of pathogens is certain to vary by bacterial strain, site of infection, prior immunity of the host, and additional factors that together merit circumspection in interpreting the broader implications of our data. Indeed, one report has described reduced clearance of *Klebsiella pneumoniae* from the lung in mice receiving statin treatment (Fessler et al., 2005), and another report, using assay conditions that would not support ETs, showed reduced opsonophagocytic killing of *S. aureus* by macrophages and GBS by HL-60 granulocytes after protracted *in vitro* treatment with simvistatin (Benati et al., 2009). Because *S. aureus* expresses an array of virulence factors that impair complement-mediated opsonphagocytosis (Jongerius et al., 2007; Laarman et al. 2010), and because it can resist oxidative burst killing through catalase expression and the antioxidant golden staphyloxanthin pigment (Liu et al., 2005), the importance of ET-dependent killing may be proportionately increased. In contrast, for pathogens highly susceptible to phagocytosis and subsequent intracellular killing mechanisms, increased stimulation of phagocytes toward the ET cell death pathway could prove inconsequential or even detrimental. Further studies of the relationship between the sterol synthesis pathways and innate immune function will be important to understand potential infectious disease ramifications for millions of individuals receiving chronic statin therapy.

EXPERIMENTAL PROCEDURES

Animals

Male 10–12 week old CD1 or C57Bl/6 mice (Charles River Laboratories, CA) were used in this study. Mice were maintained under standard conditions according to institutional guidelines. Experiments were approved by the UCSD Institutional Animal Care and Use Committee.

Bacterial Strains

The bacterial strains used in this study were *Staphylococcus aureus* strain Newman, methicillin-resistant *S. aureus* (MRSA) strain Sanger 252, *Streptococcus agalactiae* strain COH1, *Salmonella typhimurium* strain ATCC13311 and *Streptococcus pneumoniae* serotype 2 strain D39. *S. aureus, S. typhimurium and S. agalactiae strains* were grown in Todd-Hewitt broth (THB) at 37°C to mid-log phase. *S. pneumoniae* was grown in THB supplemented with 2% yeast extract (Acros). All bacteria were collected by centrifugation at 9000 rcf for 10 min, washed once with PBS and diluted to the required concentration. For pretreatment of *S. aureus* with statins, log-phase *S. aureus* Newman strain was incubated for 30 minutes in the presence of 50μM mevastatin or DMSO vehicle control. For experiments in which opsonization was used, serum was collected by spinning fresh human blood at 2000rpm for 30 minutes and collecting serum. For opsonization, log-phase *S. aureus* were incubated at 37°C in the presence of 5% human serum for 20 minutes. The bacteria were then harvested as normal. For growth curve analysis, midlog phase *S. aureus* Newman was diluted 1:100 in RPMI medium in the presence or absence of 50μM mevastatin (Sigma), 10μM YM-53601 or vehicle control (DMSO), incubated at 37°C + 5% CO_2 and bacterial density (optical density at 600 nm) was measured hourly.

Cell Culture

Human neutrophils were purified from healthy volunteers using the PolymorphPrepTM system (Axis-Shield, Fresenius) per manufacturer's recommendations. Neutrophils were cultured at 37°C + 5% CO_2 in serum-free, antibiotic-free RPMI at 10^6 cells/mL (500 μl per well in 24-well plate) in the presence of 50μM mevastatin (Sigma), 10 μM simvistatin (Sigma), 10μM GGTI-298 (Sigma), 10μM FTI-277 (Sigma), or 10μM YM-53601 with appropriate concentrations of vehicle control. After 1 h, cells were stimulated with 156ng/mL phorbol myristic acetate (PMA, Sigma) for an additional 1 h. RAW 264.7 murine and U937 human monocyte-macrophage cells were cultured at a density of 10^6 cells/mL in DMEM and RPMI 1640, respectively, supplemented with 10% heat-inactivated FBS and penicillin/streptomycin (Invitrogen). After 24 h, cells were further incubated in medium without FBS and stimulated overnight with 50μM statin or vehicle control in the presence of 50μM mevalonolactone (Sigma) to prevent apoptosis and maintain physiologic relevance.

In Vitro Bactericidal Assays

Human as well as murine cells were infected with bacteria at a MOI = 1. After centrifugation for 10 min at 1,500 rpm, infected neutrophils were incubated for 20 min at 37°C in 5% CO_2. RAW 264.7 and U937 cells were incubated for 4 and 8 h, respectively. After incubation, Triton X-100 (0.06% final concentration) was added to lyse infected cells. Lysates were diluted and plated on THA plates or THA plates supplemented with 2% yeast extract for enumeration of surviving CFU. Percent killing by statin-treated leukocytes was determined by dividing the number of CFU recovered from statin-treated neutrophils by the number of CFU from vehicle-treated neutrophils.

Phagocytosis

For determination of phagocytosis by flow cytometry, Alexa-Fluor 488-labelled *S. aureus* wood strain bioparticles (Invitrogen) were added to cells at MOI 1. After 20 min of incubation at 37°C, PMNs were washed twice with cold HBSS (Invitrogen) and mean fluorescence intensity (phagocytosis) was measured using a FACSCalibur™ flow cytometer (BD Biosciences). For infection of RAW cells, *S. aureus* bioparticles were added at MOI = 1 and centrifuged for 10 min at 1500 rpm. After an additional 10 min of incubation at 37°C, cells were washed twice with cold PBS, detached with trypsin and washed again with cold

PBS. Again, mean fluorescence intensity (phagocytosis) was measured using flow cytometry.

Oxidative Burst

After statin treatment, human neutrophils were centrifuged for 5 min at 1600 rpm and resuspended in RPMI 1640 without phenol red (Cellgro). 10μM 2′,7′ dichlorofluorescein (Sigma) was then added, and fluorescence was measured using a SpecraMAX® Gemini EM fluorescence reader over the course of one hour at 37°C. The VMax was calculated by the SpecraMAX® Pro software.

Entrapment Assay

Cells were seeded at a density of 5×10^5 cells/mL in RPMI and treated with mevastatin or vehicle control as described above to induce formation of extracellular traps. Then, cells were infected with FITC-labelled *S. aureus* strain Newman (carboxyfluorescein, Invitrogen, 30 min at 4°C) at a MOI = 20 bacteria per cell. After centrifugation for 10 min at 1,500 rpm and an additional 5 min of incubation at 37°C, cells were gently washed twice with HBSS to remove unbound bacteria. To release bacteria from extracellular traps, PMNs were incubated in the presence of 50U/mL of DNase I for 15 min at 37°C. 100μL of supernatent was transferred to a 96-well plate. Relative number of bacteria in the supernatent was determined by reading the absorption/emission at 485nm/538nm in a SpecraMAX® Gemini EM fluorescence reader (Molecular Devices).

Induction and Quantification of Extracellular Traps

To induce extracellular traps (ETs) from human PMNs, PMNs were cultured in serum-free, antibiotic-free RPMI at 10^6 cells/mL in the presence of 50 μM mevastatin (Sigma), 10 μM Simvastatin (Sigma), 50 μM Lovastatin (Sigma), 50 μM Fluvastatin (Cayman), 10 μM GGTI-298 (Sigma), 10 μM FTI-277 (Sigma), or 10 μM YM-53601 with appropriate concentrations of vehicle control. After 1 h, cells were stimulated with 156ng/mL phorbol myristic acetate (PMA, Sigma) for an additional 1h. RAW 264.7 cells were cultured at a density of 10^5 cells/mL in DMEM and RPMI 1640, respectively, supplemented with 10% heat-inactivated FBS and penicillin/streptomycin. After 4 h, cells were stimulated overnight in medium without FCS supplemented with statin (50 μM) or vehicle control and in the presence of mevalonolactone (50 μM, Sigma). To induce METs, 156 ng/mL PMA was added 2 h prior to analysis. An established method for NET quantification (Fuchs et al., 2007) was adapted for our purposes. Micrococcal nuclease (500 mU/mL, Sigma) was added to neutrophils to degrade ETs. After 15 min of incubation at 37°C, 0.5 mM EDTA was added to stop nuclease activity, and supernatants were collected. Total genomic DNA was isolated using DNAzol supplemented with polyacryl-carrier (Molecular Research Center, Inc.) per manufacturer's instructions. DNA was quantified using the PicoGreen dsDNA quantification kit (Invitrogen). Fluorescence was measured using a SpecraMAX® Gemini EM fluorescence reader. The percentage extracellular DNA was determined by dividing the amount of ET DNA by the total DNA. For peritoneal cells, 156 ng/mL PMA was added 1 h prior to analysis. ET production was assessed using a modified version on the above ET protocol. Briefly, micrococcal nuclease (500 mU/mL) was added to neutrophils to release ETs. After 15 min of incubation at 37°C, 0.5 mM EDTA was added to stop nuclease activity, and supernatants were collected. The supernatant was centrifuged for 5 minutes at 3000 rcf to remove non-adherent cells. Total genomic DNA was isolated using DNAzol supplemented with polyacryl-carrier (Molecular Research Center, Inc.) per manufacturer's instructions. DNA was quantified using the PicoGreen dsDNA quantification kit (Invitrogen). Fluorescence was measured using a SpecraMAX® Gemini EM fluorescence reader. The percentage extracellular DNA was determined by dividing the amount of ET DNA by the total DNA.

Fluorescence Microscopy

For visualization of extracellular traps, cells were seeded on poly-L-lysine coated glass-slides (neutrophils) or on glass-bottom microtiter plates (macrophages), cell-type specifically treated with statins or vehicle control as described above, infected with *S. aureus* strain Newman at a MOI of 1, centrifuged at 800 rpm for 10 min and further incubated for 20 min. The Live/Dead viability/cytotoxicity kit for mammalian cells (Invitrogen) was used without fixation of cells to visualize NETs or METs and to determine cell viability of trap-forming cells by fluorescence microscopy. Hoechst-33342-trihydrochloride (final concentration 1 μM) was added to the sample 5 min prior to microscopic analysis to stain DNA (blue). The Live/Dead BacLight™ Bacterial Viability Kit (Invitrogen) was used to determine viability of FITC-labelled *S. aureus* entrapped in the METs by fluorescence microscopy. Infected cells were stained as recommended by the manufacturer using only the red dye component to visualize dead cells, washed 3 times with PBS, fixed with 1% paraformadehyde for 5 min, washed again and mounted onto glass slides using Prolong Gold (Invitrogen), a mounting medium that contains the DNA-staining dye Dapi (blue). For immunofluorescence staining of cathelicidin peptides (murine CRAMP or human LL-37), infected cells were fixed with 4% paraformaldehyde, washed with PBS, blocked and permeabilized in the presence of PBS + 3% BSA + 2% goat serum + 0.2% TritonX100 for 45 min. Then the samples were washed again and incubated with polyclonal rabbit anti-CRAMP/LL-37 (1:300-diluted)(Dorschner et al., 2001) or with mouse monoclonal anti H2A-H2B-DNA complex (#PL2–6 mouse IgG2b stock: 2.65 mg/ml, diluted 1:3000) in the presence of PBS+2% BSA overnight at 4°C (Losman et al., 1992). A universal rabbit IgG (Dako) or mouse IgG2b (Thermo Scientific) served as isotype negative control. After washing × 3 with PBS, samples were incubated with secondary Alexa 488 or Alexa 568-labelled goat anti rabbit/mouse IgG antibodies (1:500; Molecular Probes) for 45 min at room temperature and embedded using Prolong Gold-Dapi.

Immunohistopathology

Paraffin-embedded lung tissue samples were deparafinized by immersing successively in 3 changes of xylene for 10 min each and rehydrated by immersing in decreasing concentrations of ethanol (100%, 95%, 70%, each twice for 5 min). After washing with PBS, slides were heated in a microwave for 10 min in the presence of citrate puffer (Dako) for antigen retrieval. After cooling down for 20 min, the slides were washed with PBS, and immuno-stained as described above. Mounted samples were examined using an inverted confocal laser-scanning 2-photon microscope Olympus Fluoview FV1000 with Fluoview™ Spectral Scanning technology (Olympus). Images were obtained using a 20x/0.7 or 60x/1.42 PlanApo objectives. Alternatively images were recorded using an Olympus Spinning Disc Confocal IX81 microscope with a Xenon DG5 illumination source driven by driven by SlideBook software (Intelligent Imaging Innovations). In this case, images were obtained using a 10x/0.3 UPlanFCN, 20x/0.45 LUCPlanFLN or 40x/1.0 oil UPlanApo objective. Mean fluorescence intensities of images were quantified using Image J 1.41 software.

FACS Analysis

For determination of neutrophil and macrophage content in peritoneal lavage from thioglycolate-treated mice, cells were incubated for 5 min with anti-CD32 antibodies to block Fc receptors, stained with phycoerythrin (PE)-conjugated anti-F4/80 (Serotec), fluorescein isothiocyanate (FITC) conjugated anti-Ly6G (Gr1) (BDPharmingen) or with their respective isotype control antibodies and incubated for 30 min at 4°C. Labelled cells were analyzed by flow cytometry in a FACScalibur (Becton Dickinson).

Ex Vivo Killing Assays

Outbred CD1 mice were fed ad libitum with pulverized Harlan Telkan 7912 chow +/− 500mg/kg simvastatin (generic, pharmaceutical-grade from Dr. Reddy's Laboratories Ltd.). After 5 days of feeding, mice were injected with 3mL 3% thioglycolate solution (BD Biosciences), and peritoneal cells isolated by lavage with PBS 4 h later. Cells were treated with 1x RBC lysis buffer (eBioscience) to lyse erythrocytes, resuspended in RPMI medium, and seeded in tissue culture plates at a density of 10^6 cells/mL. Cells were immediately infected with *S. aureus* strain Newman using a multiplicity of infection (MOI) = 1 and then incubated at 37°C, 5% CO_2 for 30 min. After incubation, Triton X-100 (0.06% final concentration) was added to lyse neutrophils and lysates were plated on THA for enumeration of surviving CFU.

Staphylococcus aureus Pneumonia Model

As above, outbred CD1 mice were fed ad libitum with either pulverized chow or pulverized chow supplemented with 500mg/kg simvastatin. After 5 d of feeding, mice were anesthetized with ketamine/xylazine intraperitoneally, then a sub-lethal dose of *S. aureus* strain Newman (1–2 × 10^8 CFU in 30 μl PBS) was introduced intranasally to induce pneumonia as previously described (Bubeck Wardenburg et al., 2007; Bubeck Wardenburg and Schneewind, 2008). Mice were sacrificed after 2 d, and left lung tissue was infused and preserved in 10% buffered formalin (Fisher Scientific) for histological analysis. Right lung tissue was homogenized for 1 min using zirconia beads (1 mm, Biospec) in a Mini-Beadbeater™ (BioSpec Products) and plated onto THB agar (THA) plates for overnight incubation and enumeration of colony-forming units (CFU).

Lung Histology

Formalin-fixed lung tissue was embedded in paraffin, and then cut into 3-μm-thick sections. Tissue sections were stained with hematoxylin and eosin (H&E) and then examined microscopically for pathological alterations using a Zeiss Axiolab microscope (Zeiss 10x/0.25 Achroplan, 20x/0.5 Plan-Neofluor or 40x/0.65 Achroplan objective) with an attached Sony Digital Photo 3CCD-Camera DKC-5000 at calibrated magnifications.

siRNA Transfection

To harvest thioglycolate-induced peritoneal macrophages, 12-wk old C57 Bl/6 mice were injected intraperitoneally with 3 mL of 3% thioglycolate. After 3–6 d, macrophages were harvested by peritoneal lavage with PBS and cultured in RPMI + with 10% FBS + penicillin/streptomycin. For killing assays, macrophages were cultured at 1.4×10^6 cells/mL. For extracellular trap visualization, macrophages were cultured at 5×10^5 cells/mL. Mouse Hmgcr and control SMARTpool® siRNAs (Dharmacon) were transfected into macrophages using DeliverX™ tranfection reagent (Panomics) peremanufacturer's instructions. The next day, *S. aureus* (MOI = 1) were added and brought in close proximity to macrophages by centrifugation. After 8 h of co-incubation, macrophages were lysed with 0.06% Triton X-100 and plated onto THA plates for CFU enumeration. Percent killing by Hmgcr siRNA-transfected macrophages was determined by dividing the number of CFU recovered from Hmgcr siRNA-transfected macrophages by the number of CFU from control siRNA-transfected macrophages.

Quantitative RT-PCR

Total RNA was extracted from cells using Trizol Reagent (Invitrogen). cDNA was prepared using Superscript® III First-Strand Synthesis Supermix for qRT-PCR (Invitrogen). cDNAs were amplified in SYBRR GreenER qPCR SuperMix (Invitrogen) using an ABI Prism 7100 Sequence Detection System (Applied Biosystems). We used primer sequences: Gapdh-F 5′-

AATGTGTCCGTCGTGGATCT-3′, Gapdh-R 5′-CATCGAAGGTGGAAGAGTGG-3′, Hmgcr-F 5′-TCGTCATTCATTTCCTCGACAAA-3′, Hmgcr-R 5′-GATTGCCATTCCACGAGCTAT-3′. Hmgcr sequences were taken from Primer Bank (http://pga.mgh.harvard.edu/primerbank/index.html, Primer Bank ID# 18043195a2). Cycling conditions for PCR amplifications were 15 s at 95°C, 25 s annealing at 57°C, and 45 s at 72°C. Data are expressed as relative mRNA expression levels normalized to the housekeeping gene Gapdh.

Statistics

Data were analyzed by using GraphPad Prism 4.0 (GraphPad software). Each experiment was performed at least three times at independent occasions, and within each experiment all samples were processed in triplicate. Differences were analyzed using a Student's T-test, a one-way ANOVA or a two-tailed Mann Whitney test; P values < 0.05 were considered significant.

Supplementary Material

Refer to Web version on PubMed Central for supplementary material.

Acknowledgments

This work was supported by NIH Grants AI077780 to V.N. and GM069338 to C.K.G. O.A.C. was funded in part by the UCSD Genetics Training Program (T32 GM008666). M.vK-B. was supported through a fellowship from the Deutsche Akademie der Naturforscher Leopoldina (BMBF-LPD 9901/8-187). The authors wish to thank the UCSD Histopathology Core facility and the UCSD Microscopy Facility (supported by UCSD Neuroscience Microscopy Shared Facility Grant P30 NS047101) for their assistance.

References

Almog Y, Novack V, Eisinger M, Porath A, Novack L, Gilutz H. The effect of statin therapy on infection-related mortality in patients with atherosclerotic diseases. Crit Care Med. 2007; 35:372–378. [PubMed: 17205009]

Ando H, Takamura T, Ota T, Nagai Y, Kobayashi K. Cerivastatin improves survival of mice with lipopolysaccharide-induced sepsis. J Pharmacol Exp Ther. 2000; 294:1043–1046. [PubMed: 10945857]

Bartlett AH, Foster TJ, Hayashida A, Park PW. Alpha-toxin facilitates the generation of CXC chemokine gradients and stimulates neutrophil homing in *Staphylococcus aureus* pneumonia. J Infect Dis. 2008; 198:1529–1535. [PubMed: 18823272]

Beiter K, Wartha F, Albiger B, Normark S, Zychlinsky A, Henriques-Normark B. An endonuclease allows *Streptococcus pneumoniae* to escape from neutrophil extracellular traps. Curr Biol. 2006; 16:401–407. [PubMed: 16488875]

Benati D, Ferro M, Savino MT, Ulivieri C, Schiavo E, Nuccitelli A, Pasini FL, Baldari CT. Opposite effects of simvastatin on the bactericidal and inflammatory response of macrophages to opsonized *S. aureus*. J Leukoc Biol. 2009

Bokoch GM, Prossnitz V. Isoprenoid metabolism is required for stimulation of the respiratory burst oxidase of HL-60 cells. J Clin Invest. 1992; 89:402–408. [PubMed: 1310693]

Brinkmann V, Reichard U, Goosmann C, Fauler B, Uhlemann Y, Weiss DS, Weinrauch Y, Zychlinsky A. Neutrophil extracellular traps kill bacteria. Science. 2004; 303:1532–1535. [PubMed: 15001782]

Brinkmann V, Zychlinsky A. Beneficial suicide: why neutrophils die to make NETs. Nat Rev Microbiol. 2007; 5:577–582. [PubMed: 17632569]

Bubeck Wardenburg J, Patel RJ, Schneewind O. Surface proteins and exotoxins are required for the pathogenesis of *Staphylococcus aureus* pneumonia. Infect Immun. 2007; 75:1040–1044. [PubMed: 17101657]

Bubeck Wardenburg J, Schneewind O. Vaccine protection against *Staphylococcus aureus* pneumonia. J Exp Med. 2008; 205:287–294. [PubMed: 18268041]

Buchanan JT, Simpson AJ, Aziz RK, Liu GY, Kristian SA, Kotb M, Feramisco J, Nizet V. DNase expression allows the pathogen group A *Streptococcus* to escape killing in neutrophil extracellular traps. Curr Biol. 2006; 16:396–400. [PubMed: 16488874]

Catron DM, Lange Y, Borensztajn J, Sylvester MD, Jones BD, Haldar K. *Salmonella enterica* serovar Typhimurium requires nonsterol precursors of the cholesterol biosynthetic pathway for intracellular proliferation. Infect Immun. 2004; 72:1036–1042. [PubMed: 14742551]

Chaudhry MZ, Wang JH, Blankson S, Redmond HP. Statin (cerivastatin) protects mice against sepsis-related death via reduced proinflammatory cytokines and enhanced bacterial clearance. Surg Infect (Larchmt). 2008; 9:183–194. [PubMed: 18426351]

Crotty Alexander LE, Maisey HC, Timmer AM, Rooijakkers SH, Gallo RL, von Kockritz-Blickwede M, Nizet V. M1T1 group A streptococcal pili promote epithelial colonization but diminish systemic virulence through neutrophil extracellular entrapment. J Mol Med. 2010; 88:371–381. [PubMed: 19960175]

Dorschner RA, Pestonjamasp VK, Tamakuwala S, Ohtake T, Rudisill J, Nizet V, Agerberth B, Gudmundsson GH, Gallo RL. Cutaneous injury induces the release of cathelicidin anti-microbial peptides active against group A *Streptococcus*. J Invest Dermatol. 2001; 117:91–97. [PubMed: 11442754]

Fessler MB, Young SK, Jeyaseelan S, Lieber JG, Arndt PG, Nick JA, Worthen GS. A role for hydroxy-methylglutaryl coenzyme a reductase in pulmonary inflammation and host defense. Am J Respir Crit Care Med. 2005; 171:606–615. [PubMed: 15591471]

Fuchs TA, Abed U, Goosmann C, Hurwitz R, Schulze I, Wahn V, Weinrauch Y, Brinkmann V, Zychlinsky A. Novel cell death program leads to neutrophil extracellular traps. J Cell Biol. 2007; 176:231–241. [PubMed: 17210947]

Gupta AK, Joshi MB, Philippova M, Erne P, Hasler P, Hahn S, Resink TJ. Activated endothelial cells induce neutrophil extracellular traps and are susceptible to NETosis-mediated cell death. FEBS Lett. 2010; 584:3193–3197. [PubMed: 20541553]

Hakkim A, Furnrohr BG, Amann K, Laube B, Abed UA, Brinkmann V, Herrmann M, Voll RE, Zychlinsky A. Impairment of neutrophil extracellular trap degradation is associated with lupus nephritis. Proc Natl Acad Sci U S A. 107:9813–9818. [PubMed: 20439745]

Jerwood S, Cohen J. Unexpected antimicrobial effect of statins. J Antimicrob Chemother. 2008; 61:362–364. [PubMed: 18086693]

Jongerius I, Kohl J, Pandey MK, Ruyken M, van Kessel KP, van Strijp JA, Rooijakkers SH. Staphylococcal complement evasion by various convertase-blocking molecules. J Exp Med. 2007; 204:2461–2471. [PubMed: 17893203]

Kessenbrock K, Krumbholz M, Schonermarck U, Back W, Gross WL, Werb Z, Grone HJ, Brinkmann V, Jenne DE. Netting neutrophils in autoimmune small-vessel vasculitis. Nat Med. 2009; 15:623–625. [PubMed: 19448636]

Kobayashi SD, Braughton KR, Palazzolo-Ballance AM, Kennedy AD, Sampaio E, Kristosturyan E, Whitney AR, Sturdevant DE, Dorward DW, Holland SM, et al. Rapid neutrophil destruction following phagocytosis of *Staphylococcus aureus*. J Innate Immun (online early). 201010.1159/000317134

Kopterides P, Falagas ME. Statins for sepsis: a critical and updated review. Clin Microbiol Infect. 2009; 15:325–334. [PubMed: 19416304]

Kruger P, Fitzsimmons K, Cook D, Jones M, Nimmo G. Statin therapy is associated with fewer deaths in patients with bacteraemia. Intensive Care Med. 2006; 32:75–79. [PubMed: 16283159]

Laarman A, Milder F, van Strijp J, Rooijakkers S. Complement inhibition by gram-positive pathogens: molecular mechanisms and therapeutic implications. J Mol Med. 88:115–120. [PubMed: 20062962]

Liappis AP, Kan VL, Rochester CG, Simon GL. The effect of statins on mortality in patients with bacteremia. Clin Infect Dis. 2001; 33:1352–1357. [PubMed: 11565076]

Liu GY, Essex A, Buchanan JT, Datta V, Hoffman HM, Bastian JF, Fierer J, Nizet V. *Staphylococcus aureus* golden pigment impairs neutrophil killing and promotes virulence through its antioxidant activity. J Exp Med. 2005; 202:209–215. [PubMed: 16009720]

Losman MJ, Fasy TM, Novick KE, Monestier M. Monoclonal autoantibodies to subnucleosomes from a MRL/Mp(−)+/+ mouse. Oligoclonality of the antibody response and recognition of a determinant composed of histones H2A, H2B, and DNA. J Immunol. 1992; 148:1561–1569. [PubMed: 1371530]

Martin CP, Talbert RL, Burgess DS, Peters JI. Effectiveness of statins in reducing the rate of severe sepsis: a retrospective evaluation. Pharmacotherapy. 2007; 27:20–26. [PubMed: 17192158]

Merx MW, Liehn EA, Graf J, van de Sandt A, Schaltenbrand M, Schrader J, Hanrath P, Weber C. Statin treatment after onset of sepsis in a murine model improves survival. Circulation. 2005; 112:117–124. [PubMed: 15998696]

Merx MW, Liehn EA, Janssens U, Lutticken R, Schrader J, Hanrath P, Weber C. HMG-CoA reductase inhibitor simvastatin profoundly improves survival in a murine model of sepsis. Circulation. 2004; 109:2560–2565. [PubMed: 15123521]

Merx MW, Weber C. Benefits of statins beyond lipid lowering. Drug Discov Today Dis Mech. 2008; 5:325–331.

Niessner A, Steiner S, Speidl WS, Pleiner J, Seidinger D, Maurer G, Goronzy JJ, Weyand CM, Kopp CW, Huber K, et al. Simvastatin suppresses endotoxin-induced upregulation of toll-like receptors 4 and 2 in vivo. Atherosclerosis. 2006; 189:408–413. [PubMed: 16443229]

Nugent KM, Pesanti EL. Nonphagocytic clearance of *Staphylococcus aureus* from murine lungs. Infect Immun. 1982; 36:1185–1191. [PubMed: 7095846]

Pahan K, Sheikh FG, Namboodiri AM, Singh I. Lovastatin and phenylacetate inhibit the induction of nitric oxide synthase and cytokines in rat primary astrocytes, microglia, and macrophages. J Clin Invest. 1997; 100:2671–2679. [PubMed: 9389730]

Rosenson RS, Tangney CC, Casey LC. Inhibition of proinflammatory cytokine production by pravastatin. Lancet. 1999; 353:983–984. [PubMed: 10459915]

Stagnitti MN. Trends in statins utilization and expenditures for the U.S. civilian noninstitutionalized population, 2000 and 2005. Statistical Brief. 2008:205.

Thelen KM, Rentsch KM, Gutteck U, Heverin M, Olin M, Andersson U, von Eckardstein A, Bjorkhem I, Lutjohann D. Brain cholesterol synthesis in mice is affected by high dose of simvastatin but not of pravastatin. J Pharmacol Exp Ther. 2006; 316:1146–1152. [PubMed: 16282522]

Thomsen RW, Riis A, Kornum JB, Christensen S, Johnsen SP, Sorensen HT. Preadmission use of statins and outcomes after hospitalization with pneumonia: population-based cohort study of 29,900 patients. Arch Intern Med. 2008; 168:2081–2087. [PubMed: 18955636]

Urban CF, Reichard U, Brinkmann V, Zychlinsky A. Neutrophil extracellular traps capture and kill *Candida albicans* yeast and hyphal forms. Cell Microbiol. 2006; 8:668–676. [PubMed: 16548892]

von Kockritz-Blickwede M, Goldmann O, Thulin P, Heinemann K, Norrby-Teglund A, Rohde M, Medina E. Phagocytosis-independent antimicrobial activity of mast cells by means of extracellular trap formation. Blood. 2008; 111:3070–3080. [PubMed: 18182576]

von Kockritz-Blickwede M, Nizet V. Innate immunity turned inside-out: antimicrobial defense by phagocyte extracellular traps. J Mol Med. 2009; 87:775–783. [PubMed: 19444424]

Walker MJ, Hollands A, Sanderson-Smith ML, Cole JN, Kirk JK, Henningham A, McArthur JD, Dinkla K, Aziz RK, Kansal RG, et al. DNase Sda1 provides selection pressure for a switch to invasive group A streptococcal infection. Nat Med. 2007; 13:981–985. [PubMed: 17632528]

Wang Y, Li M, Stadler S, Correll S, Li P, Wang D, Hayama R, Leonelli L, Han H, Grigoryev SA, et al. Histone hypercitrullination mediates chromatin decondensation and neutrophil extracellular trap formation. J Cell Biol. 2009; 184:205–213. [PubMed: 19153223]

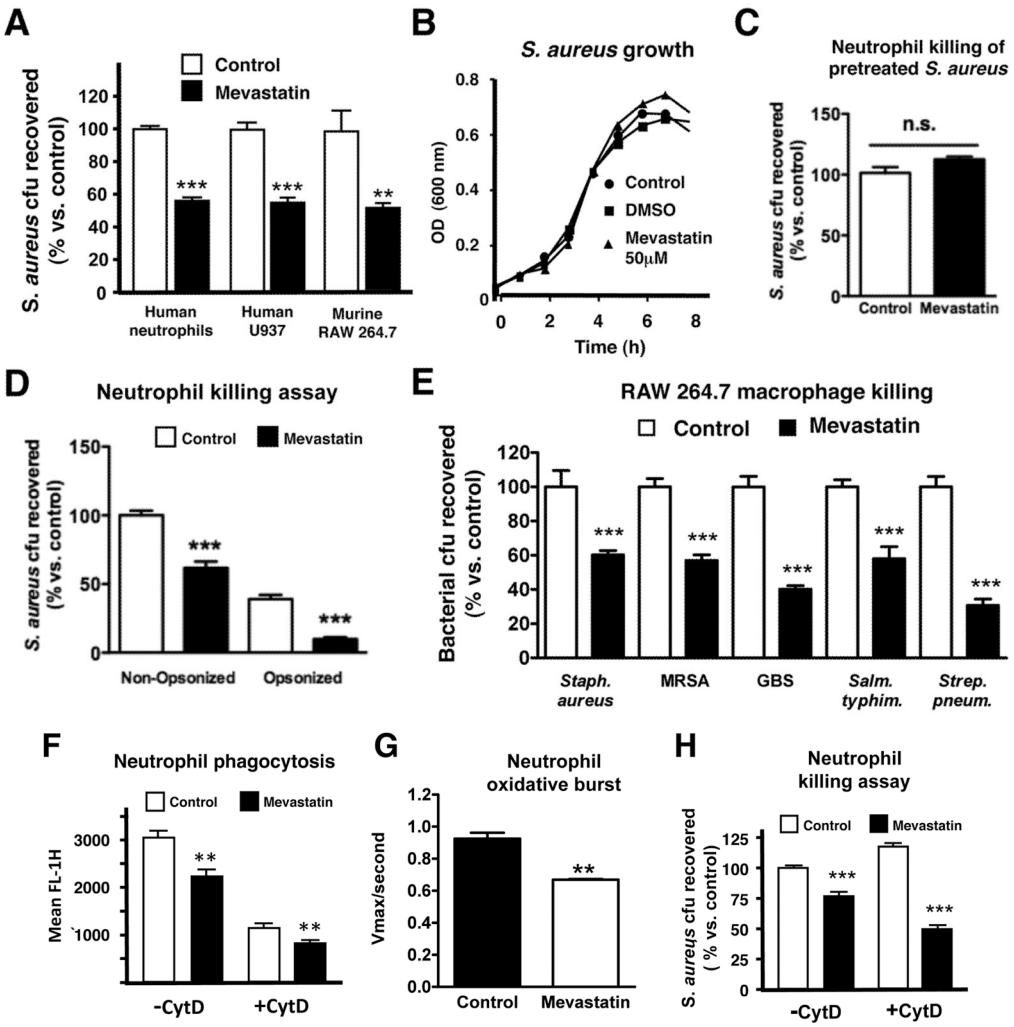

Figure 1. Statin Induction of Phagocyte Antimicrobial Activity *In Vitro*

(A) *In vitro* killing of *S. aureus* by primary human neutrophils or RAW 264.7 and human U937 cells treated with mevastatin or vehicle control. (B). Growth of *S. aureus* strain Newman in RPMI with or without mevastatin (50 μM) or DMSO vehicle control. (C) *In vitro* killing of *S. aureus* pretreated with mevastatin or vehicle control by primary human neutrophils. (D) *In vitro* killing of opsonized versus non-opsonized *S. aureus* by primary human neutrophils treated with mevastatin or vehicle control. (E) *In vitro* killing of *S. aureus* strain Newman, *S. aureus* strain Sanger (MRSA), *S. agalactiae* strain COH1 (GBS), *S. typhimurium* and *Streptococcus pneumoniae* strain D39 by RAW 264.7 cells treated with mevastatin or vehicle control. (F) Mean fluorescence intensity as parameter for phagocytosis of neutrophils after infection with FITC-labelled *S. aureus* Wood strain bioparticles measured by flow cytometry. As a control, 10 μg/ml of cytochalasin D was added to the samples 10 min prior to infection to prevent phagocytosis. (G) Oxidative burst of primary human neutrophils stimulated with mevastatin or vehicle control measured by flow cytometry after 30 min incubation in the presence of 2′,7′ dichlorofluorescein. (H) Extracellular killing of *S. aureus* by primary human neutrophils treated with mevastatin or vehicle control. To prevent phagocytosis, 10 μg/ml of cytochalasin D was added to the samples 10 min prior to infection. Experiments performed 3–4 times with similar results,

representative experiment shown ± standard deviation. ** $P < 0.01$, *** $P < 0.005$, n.s. = not significant by two-tailed Student's t-test comparing control versus statin-treated group.

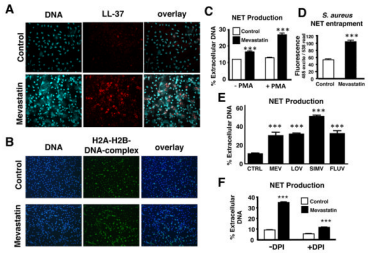

Figure 2. Statin Induction of Neutrophil Extracellular Traps (NETs)

(A) Representative fluorescent images of neutrophils stimulated with mevastatin or vehicle control and PMA to induce NETs. NET-formation was visualized in blue (Dapi) and LL-37 expression was visualized by Alexa red-immunostaining. (B) NET-formation was visualized in blue (Dapi) and H2A-H2B-DNA-complexes were visualized by Alexa green-immunostaining. (C) Quantification of NET-production by primary human neutrophils ± stimulation with PMA and treatment with mevastatin or vehicle control. (D) Entrapment of fluorescently labeled *S. aureus* by PMA-stimulated human neutrophils treated with mevastatin or vehicle control. In (C-D) *** $P < 0.005$ by two-tailed Student's t-test comparing control versus statin-treated group. (E) Quantification of NET-production by primary human neutrophils ± stimulation with PMA and treatment with different statins (MEV = mevastatin, LOV = lovastatin, SIMV = simvastatin, FLUV = fluvastatin) or vehicle control (CTRL). *** $P < 0.005$ by one-way ANOVA with Dunnet's post-test vs. control group. (F) NET production of PMA-stimulated human neutrophils treated with 10 μg/ml DPI or vehicle control to inhibit the NADPH-oxidase-dependent ROS production. *** $P < 0.005$ or n.s. = not significant by two-tailed Student's t-test comparing control versus statin-treated group. Experiments performed 3–4 times with similar results, representative experiment shown ± standard deviation. (See also the Supplemental Figures S1 and S2)

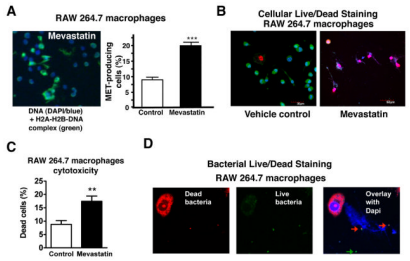

Figure 3. Statin-Induced Formation of Macrophage Extracellular Traps (METs)

(A) MET formation by RAW 264.7 cells. Representative fluorescent image of MET formation visualized using blue (Dapi) and Alexa green-immunostaining for H2A-H2B-DNA-complexes; quantification of MET production by RAW 264.7 cells after overnight treatment with mevastatin or vehicle control and subsequent stimulation with PMA. Experiment was performed at 3 independent occasions with similar results, representative experiment shown ± standard deviation. *** $P < 0.005$ by t-test; (B) Live/Dead viability/cytotoxicity staining to determine viability of MET-producing cells or (C) Live/Dead BacLight™ Bacterial Viability staining to determine viability of FITC-labelled *S. aureus* entrapped in the METs produced by RAW cells after overnight treatment with mevastatin and subsequent stimulation with PMA. Note that all trap-forming macrophages as well as entrapped bacteria are dead as shown by the red dye (arrows); non-entrapped bacteria are not stained by the red dye (green arrow) indicating that they are alive. (See also the Supplemental Figures S3 and S4).

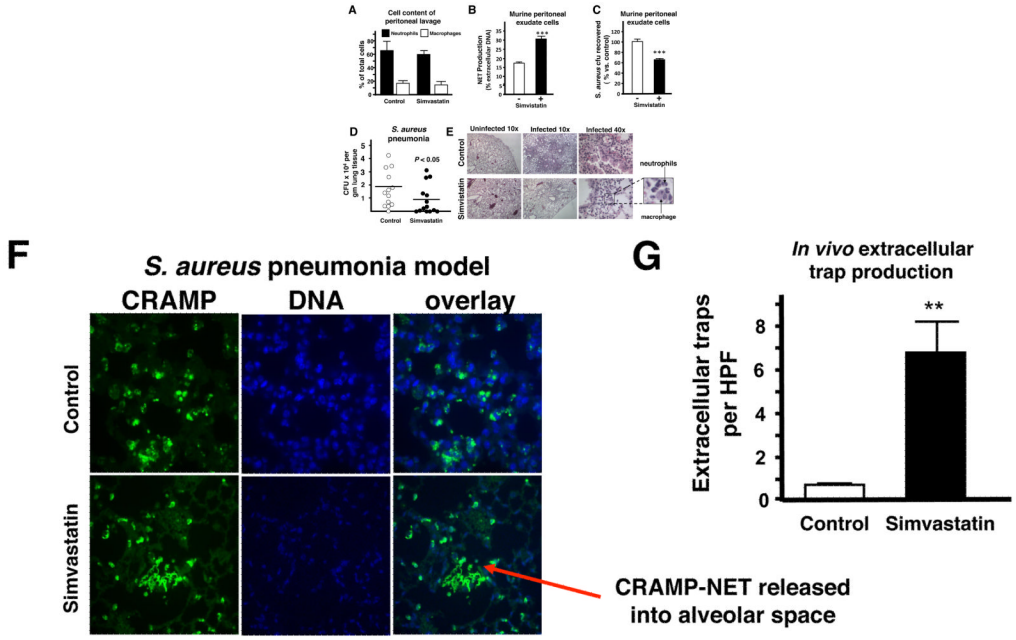

Figure 4. Statin Therapy in Mice Boosts Extracellular Trap Formation *Ex Vivo* and *In Vivo*

(A) Cell content (percentage of total cells) of thioglycolate-induced peritoneal cells extracted from mice fed with standard chow or standard chow + simvastatin. (B) Quantification of NET production by peritoneal cells. (C) *Ex vivo* killing of *S. aureus* strain Newman by thioglycolate-induced peritoneal cells extracted from mice fed with standard chow or standard chow + simvastatin. In (B–C): *** $P < 0.005$ by two-tailed Student'st-test comparing control versus statin-treated group. Experiments performed 3–4 times with similar results, representative experiment shown ± standard deviation. (D) Recovered bacteria from lungs of mice pre-fed for with standard chow or standard chow supplemented with simvastatin and infected intranasally with 2×10^8 CFU *S. aureus* strain Newman for 48 h. Data shown are pooled from 2 independent experiments with each n = 10 or n = 7 mice, respectively. * $P < 0.05$ by two-tailed Mann Whitney test. (E) Representative light micrograph (HE-stained) of lung tissue sections of infected mice pre-fed for with standard chow (control, upper panel) or standard chow supplemented with simvastatin (lower panel). (F) Representative fluorescent images of extracellular trap formation (visualized by Alexa 488 (green)-labelled CRAMP production and counterstained with Dapi) in paraffin-embedded lung sections of mice pre-fed for with standard chow or standard chow supplemented with simvastatin and intranasally infected with 2×10^8 cfu of *S. aureus* strain Newman for 48 h. (G) Quantification of *in vivo* extracellular trap production visualized in (F). Data are shown as average of 6 high-power field (HPF) obtained with a 10x/0.3 UPlanFCN objective. ** $P < 0.01$ by two-tailed Student's t-test. (See also the Supplemental Figure S5).

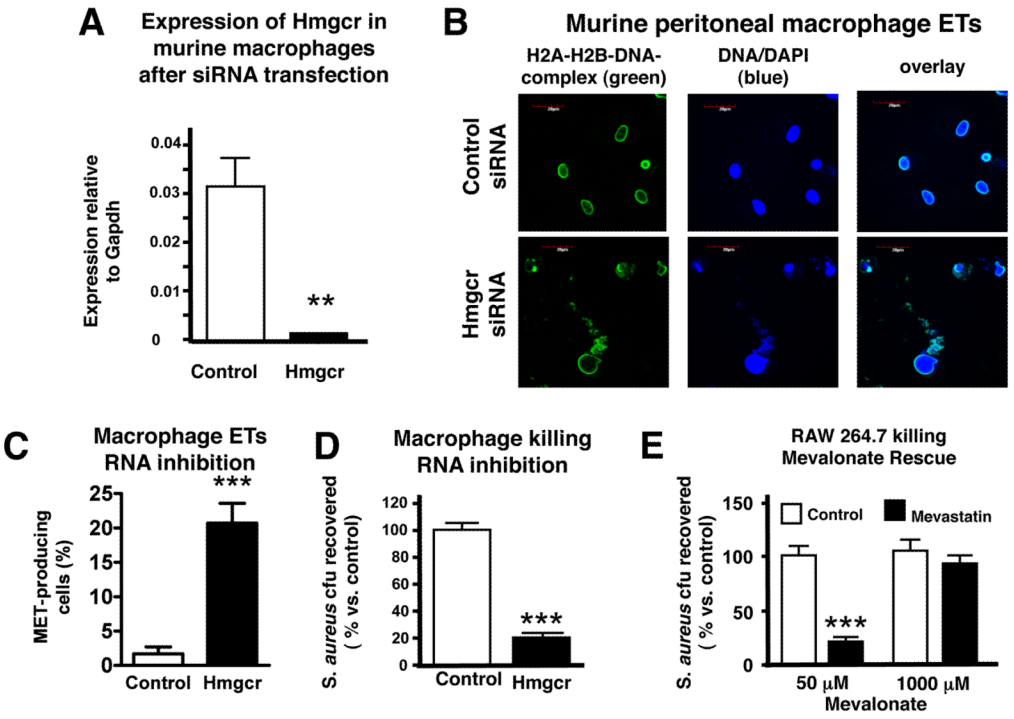

Figure 5. Statin Induction of Extracellular Traps Involves HMG-CoA Reductase Inhibition

(A) Hmgcr transcript expression in thioglycolate-induced macrophages transfected with Hmgcr siRNA. (B) Representative fluorescent images of murine thioglycolate-induced peritoneal macrophages following transfection with Hmgcr or control siRNA forming extracellular traps. MET-formation was visualized in blue (Dapi) and H2A-H2B-DNA-complexes were visualized by Alexa green-immunostaining. (C) Quantification of MET production by murine thioglycolate-induced peritoneal macrophages following transfection with Hmgcr or control siRNA. (D) Killing of *S. aureus* by murine thioglycolate-induced peritoneal macrophages following transfection with Hmgcr or control siRNA. (E) Killing of *S. aureus* by RAW 264.7 cells following treatment with mevastatin or vehicle control ± mevalonate. * $P < 0.05$, ** $P < 0.01$, *** $P < 0.005$ by two-tailed Student's t-test comparing control versus statin-treated group. Experiments performed 3–4 times with similar results, representative experiment shown ± standard deviation. (See also the Supplemental Figures S6).

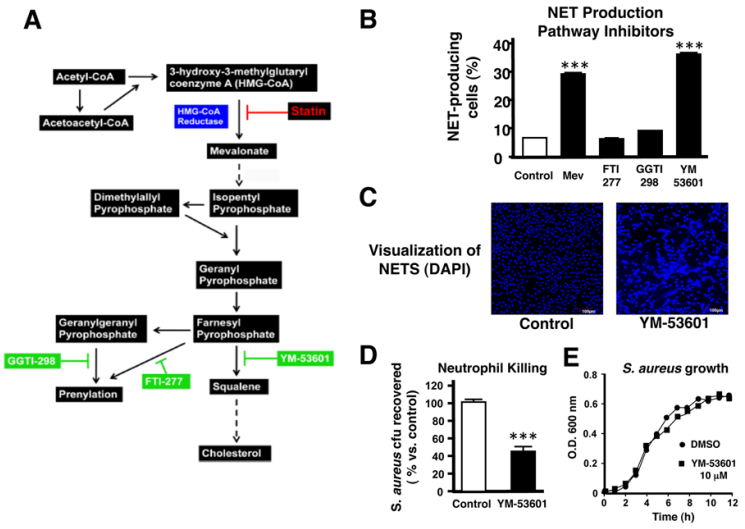

Figure 6. Neutrophil Extracellular Trap Induction Involves the Sterol Synthesis Pathway

(A) Diagram of the mevalonate pathway. (B) Neutrophil extracellular trap (NET) production following treatment of primary human neutrophils with inhibitors of the mevalonate pathway. *** $P < 0.005$ by one-way ANOVA with Dunnet post-test versus control group. (C) Representative fluorescent images of NET formation by human primary neutrophils in response to YM-53601 or vehicle control treatment visualized by DAPI staining. (D) Killing of *S. aureus* by human neutrophils following treatment with YM-53601 or vehicle control. *** $P < 0.005$ by two-tailed Student's t-test comparing control versus statin-treated group. (E) Growth of *S. aureus* strain Newman in RPMI containing YM-53601 (10 μM) or DMSO vehicle control. Experiments performed 3–4 times with similar results, representative experiment shown ± standard deviation.